Journal of Petroleum Exploration and Production Technology (2021) 11:3859–3878
https://doi.org/10.1007/s13202-021-01266-3

ORIGINAL PAPER-PRODUCTION ENGINEERING

Optimal operation of a multi-distribution natural gas pipeline grid: an ant colony approach

Adarsh Kumar Arya[1]

Received: 11 May 2021 / Accepted: 17 August 2021 / Published online: 25 August 2021

Abstract

The enormous cost of transporting oil and gas through pipelines and the operational benefits that the industry receives through optimization has incited analysts for decades to find optimization strategies that help pipeline managers operate pipeline grids with the least expense. The paper aims to minimize the pipeline grids' operating costs using an ant colony optimization strategy. The article constructs a multi-objective modeling framework for a natural gas pipeline grid based on data from the French gas pipeline network corporation 'Gaz De France,' using pipeline and compressor hydraulics. The gas pipeline grid comprises seven gas supply nodes and nineteen gas distribution centers. Seven compressor stations provided at various locations on the pipeline route raise the gas pressure. Two competing objectives of reducing fuel usage in compressors and increasing throughput at distribution centers are acknowledged to reduce the pipeline's operating cost. The 'multi-objective ant colony optimization (MOACO)' approach is implemented to the pipeline transportation model to reduce the natural gas pipeline grid's operating cost. The process variables include the amount of gas flowing through the pipe and the pressure at pipe nodes. This method provides the optimum solution for each fuel consumption level on each compressor, and it does so by producing a Pareto front for each of the nineteen gas distribution points. The blueprints of the methodology used and the findings collected intend to guide pipeline managers and select the best of the most preferred solutions.

Keywords Gas hydraulics · Multi-objective optimization · Ant colony optimization · Natural gas · Pipeline

List of Symbols

d_e	Density of gas (kg/m^3)
D	Pipeline diameter (m)
e	Absolute roughness
f	Friction factor(dimensionless)
h	Isentropic head across compressors (KJ/kg)
H_m	Heat content of gas mixture (J/kg)
γ	Isentropic exponent
L	Length of pipe segment (m)
M	Mass flow rate of gas in pipe arc(kg/sec)
m_f	Mass of fuel consumed in compressors(kg/sec)
m_s	Gas supply rate(kg/sec)
m_{de}	Gas delivery rate
M_{NG}	Molecular weight of natural gas
MAOP	Maximum allowable operating pressure
η_p	Polytropic exponent
η_m	Mechanical efficiency
P_b	Base pressure (bar)
P_c	Critical pressure (bar)
P_s	P_d, suction and discharge pressure (bar)
P_{sd}	Average pressure (bar)
q	Volumetric flow rate (m^3/sec)
Q_{base}	Volumetric flow rate at std. conditions (m3/sec)
R	Gas constant (m^3.kPa/ kmol.K)
S	Specified minimum yield stress(bar)
Tb	Base temperature(K)
t	Thickness of pipeline(m)
V	Velocity of gas(m/sec)
y	Mole fraction
z	Compressibility factor
η_{dr}	Driver efficiency
η_{is}	Isentropic efficiency
s	Elevation factor

✉ Adarsh Kumar Arya
akarya@ddn.upes.ac.in

[1] Department of Chemical Engineering, School of Engineering, University of Petroleum and Energy Studies, Energy Acres Building, Bidholi, Dehradun 248007, India

Introduction

Energy usage has grown exponentially worldwide over the last few decades. Energy consumption growth has been almost 50% (OECD, 2012). The vast energy demand has put extreme pressure on exploring industries to provide an economical energy source. The government's various environmental regulations on the industrial sectors to minimize greenhouse gas emissions have also expressed the need for a cleaner energy source. These circumstances have led to wider natural gas consumption than other fossil fuels to satisfy the energy hunger economy. International Emergency Agency claims that the planet has enough natural gas supplies that can comfortably last 230 years more (IEA, 2012). Compared to other fossil fuels, natural gas has the advantage that it is environmentally friendly, safer, and easier to store. Natural gas usage is versatile. It has numerous applications as a fuel supply for automobiles and a chemical feedstock to produce plastics and other economically significant organic chemicals (Guo, 2005). Natural gas-fired power plants start and stop much less frequently than those operated by coal. Natural gas is consistent with alternative energy options, such as solar and wind, which only exist during sunlight or wind blows. All these factors have revoked industries to exploit the benefits of natural gas.

The demand for natural gas has been much higher in developing nations like India and China. In the last twenty years, natural gas demand has increased threefold in India and ninefold in China. The gas demand is likely to increase by 37% by 2030 (B.P 2013).

The increase in natural gas utilization in various sectors requires a carefully and intelligently designed gas production infrastructure. Pipelines remain in use for the transportation of oil and gas for decades. Compared to other transportation modes, pipelines have the advantages of low cost, lesser GHG emission, low energy consumption, continuous supply, safer, lesser maintenance, and easiness in transportation under challenging terrains. These factors make pipelines an exceptional mode for transporting oil and gas (Thakur et al. 2020; Thakur & Arya, 2021). Pipelines comprise many short to medium-length pipes, pumps, fittings, compressors, and regulators. Pipelines experience high-pressure changes due to uneven terrain and friction caused by gas molecules interacting with the pipeline walls. Compressor stations help raise the gas pressure in the pipeline. Natural gas, used as fuel in compressors, provides the energy necessary to operate the compressors.

Researchers found that compressors consume three to five percent of gas flowing through the pipeline (Wu S et al. 2000). Since pipelines transport large amounts of gas, a loss of 3–5 percent gas is immense. The loss of gas may account for 25–30% of the total company's operating budget (Demissie and Zhu, 2017). A minimal saving of only 1% of the total fuel consumed may save 5 million dollars per year (Carter, 1996). Improvement in the pipeline grid performance by reducing fuel consumption is critical (Arya AK, 2015). The other big challenge we face is reducing energy consumption in the compressor and improving gas throughput simultaneously—the paper studies the optimum gas distribution to maximize the throughput at minimal fuel consumption.

Review on optimization parameters and optimization techniques

Researchers are trying to find the most profitable optimization methods for pipeline grid operation. There is already an extensive literature review published (Zheng et al. 2010; Hamedi, Farahani, and Esmaeilian, 2011; Rios-Mercado and Borraz-Sanchez, 2015; Demissie and Zhu, 2015). The following section gives an overview of optimization parameters and the techniques used to optimize those pipeline parameters.

Review of gas pipeline optimization parameters

Researchers have made numerous efforts to optimize gas pipeline grids. Several operational parameters are reported in the literature to maximize the pipeline's operational benefits (Ríos-Mercado, 2015). Design and operational parameters are common to optimization decisions (Demissie et al. 2017; Guerra et al. 2016). In the design optimization problems, the research focuses on the pipeline structure such as optimal sizing of pipes (Boyd et al. 1994), the material selection of pipeline, number and position of compressors (Edger and Himmelblau, 2001), the distance between compressors, and future expansion of pipelines (Uster and Dilaveroglu, 2014). The primary objective of design optimization is to maximize the transmission power of the pipeline (Alves, Souza, and Costa, 2016), increase the flexibility in the operation of the pipeline (Fodstad, Midthun, and Tomasgard, 2015), and account for future expansion plan with minimum investment cost (Mikolajková et al. 2017). Pipeline optimization parameters include maximizing the line pack of pipelines (Alinia et al. 2014), maximizing the throughput of gas (Fasihizadeh et al. 2014), minimizing fuel consumption (Arya and Honwad, 2015), and minimizing greenhouse gas emissions (Yang et al. 2017).

Review of gas pipeline optimization techniques

The design and operational pipeline parameters are highly complex, including nonlinear and non-differential functions because of the objective function's non-convex nature. Numerous optimization algorithms have been analyzed extensively in the last few decades. Classical (deterministic) and stochastic (evolutionary) approaches are the two methodologies for pipeline optimization (Arya & Honwad, 2015). Dynamic programming (Wong and Larsen, 1968; Osiadacz, 1994; Carter, 1998), generalized reduced gradient (Adeyuanju and Oyekunle 2004; Tabkhi 2007), and linear programming methods are the most common classical methods extensively used for pipeline optimization. The principle of dynamic programming has proven to be the most effective approach for deriving algorithms. These techniques can ease the ability to handle the nonlinearity of the objective function.

The dynamic programming technique does not get stuck searching for the global optimum. The technique, however, has the drawback of high computational time for complex grids. Most real case pipeline grids are highly complex, having numerous pipes, compressors, supply, and delivery points. In those cases, the technique becomes almost obsolete, as the time required to achieve the optimum solution is almost infeasible. The general gradient technique functions well with complex pipeline grids. However, these techniques depend on gradient search methods and hence have the drawback that they fail if the function is non-differentiable and discontinuous. In these cases, the solution obtained is easily trapped in local optima and cannot further optimize the grid. Linear programming methods can find the global optimum but works only when the objective function is nearly linear. The solution obtained in classical methods essentially depends on the initial value chosen.

Moreover, all the mentioned classical techniques deal only with nonlinear programming (NLP) problems. These methods struggle when dealing with a nonlinear problem (MINLP). Researchers are now focusing on stochastic algorithms or evolutionary algorithms to deal with these kinds of issues. These algorithms have the advantage that they can deal with large-scale problems and are capable of solving MINLP problems (Elbeltagi et al. 2005). Stochastic approaches focus on the creation of or social actions of living organisms. The species in these algorithms search the solution boundary based on individual samples rather than gradient information. Hence, they are not dependent on gradient information. Besides, these methods adapt to discrete variables quickly. Literature reports numerous stochastic techniques. The most popular ones used for pipeline optimization are genetic algorithms (Goldberg and Kuo, 1985; Montoya, 2000; Molaei, 2007; Hawryluk, 2010), particle swarm optimization (Xia et al. 2020), simulated annealing (Wright et al. 1988), differential evolution (Qin et al. 2009), artificial neural grids (Mohamadi Baghmolaei 2014), and ant colony algorithms (Arya and Honwad, 2018a; Arya and Honwad, 2018b). Among all these methods, ACO methods can respond quickly in less time to complex changes.

Previously multi-objective ant colony optimization (ACO) technique has been extended to a barrel grid (Arya and Honwad, 2018a). Some of the work on a similar objective was carried out by Chebouba A, 2015; Demissie and Zhu, 2017; Osiadacz and Isoli, 2020. The technique, however, has not been applied to a typical multi-distribution pipeline grid. The present paper develops a multi-objective gas pipeline model for a multi-distribution grid and further optimizes it using the MOACO method.

Analysis of the gas pipeline grid

The present section first states the various assumptions applied while modeling the pipeline grid. Pipeline and compressor simulation equations are discussed further in the section.

Pipeline grid assumptions

The following assumptions are used while modeling the gas pipeline grid.

Steady state

In the actual scenario, the gas flow is transient (unsteady), which means that the fluid properties of gas change with time. However, consideration of transient conditions leads to increased variables and further complexity in handling the problem. For simplifying the problem and get the results in real time, the paper assumes steady-state conditions. In most cases, considering steady-state conditions in a natural gas pipeline grid leads to acceptable results and deviates very little from the real situations (Osiadacz and Chaczykowski, 2001).

Flow direction

The gas flow has a been pre-specified direction.

Isothermal flow

The gas's heat flow to the surrounding environment decreases the gas temperature over the pipeline's length. However, pipelines are long entities that carry oil and gas to very long distances. In these cases, the gas's temperature

quickly acquires the surrounding temperature and becomes constant (Menon, 2005). Hence, in the present paper, the gas temperature is assumed constant at 298 K.

Compressor type

Centrifugal compressors relatively require less maintenance and are cheaper than reciprocating.

pumps. The present paper assumes that all the compressors are of a centrifugal type.

Adiabatic compression

The paper assumes an adiabatic compression process.

Pipeline grid description

Figure 1 portrays a multi-distribution natural gas grid captured from a French gas distribution firm 'Gaz De France.' The grid holds thirty pipe arcs that link six supply stations to nineteen distribution stations. The pipeline grid consists of seven compressor stations that raise the gas pressure. Forty-five nodes constitute the entire pipeline grid. It includes six gas supply nodes connected to nineteen distribution nodes through twenty intermediate nodes. There are ten control valves installed in the pipe network to do double or triple controls on the outputs of three or more different stages of the compressor; they are either placed after compressors on one side of the system to break up the outputs or used in two or three parallel pipes to increase

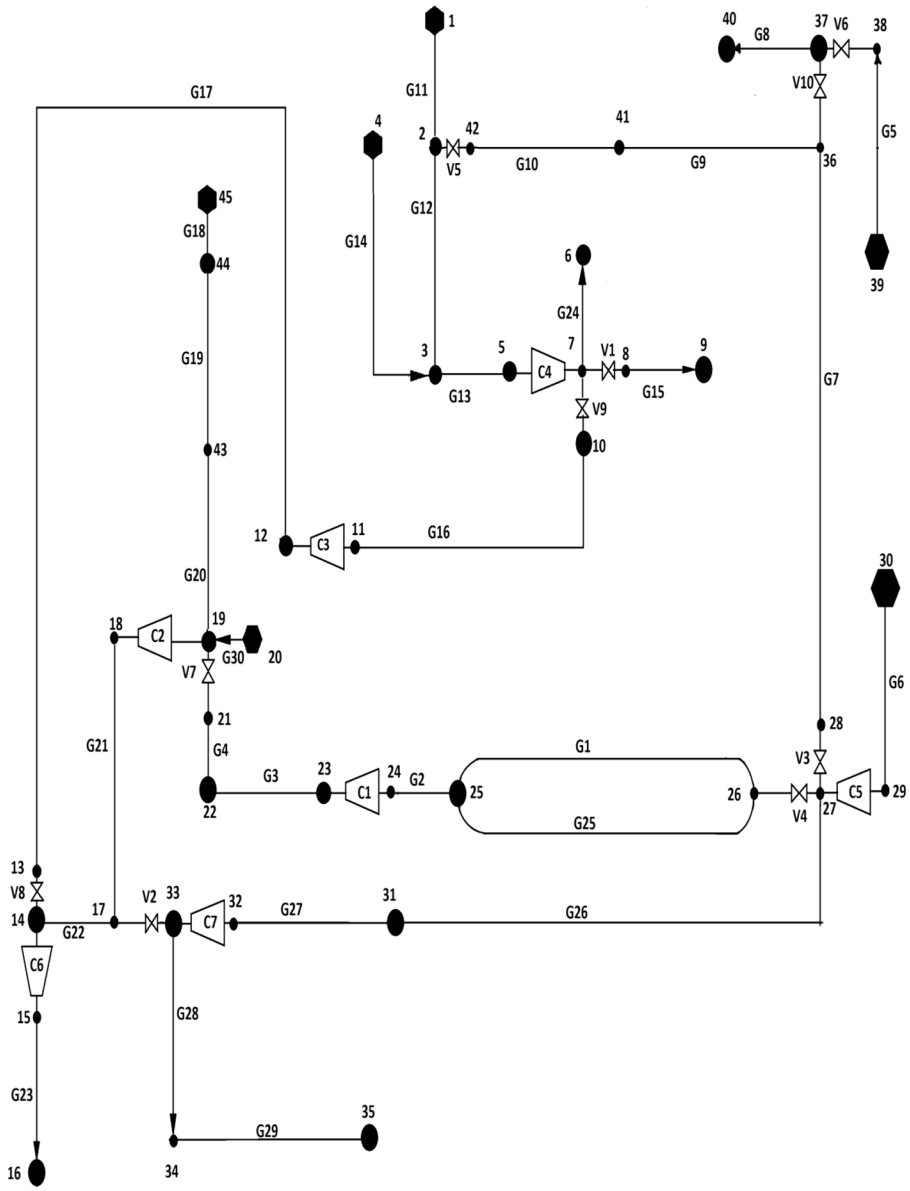

Fig. 1 Multi-distribution gas pipeline network system (Arya 2018)

Table 1 Features of Pipe Arcs (Tabkhi, 2007)

Pipe Arc	Symbol	Diameter (mm)	Length (Km)	MAOP (Bar)	Upstream and downstream nodes	Roughness (μm)
1	G_1	754	64.1	68	26–25	20
2	G_2	688	101.6	68	25–24	20
3	G_3	681	80.4	68	23–22	10
4	G_4	617	27.1	68	22–21	10
5	G_5	1090	172.699	85	39–38	10
6	G_6	1167	4.9	68	30–29	10
7	G_7	1069	122.2	68	28–36	10
8	G_8	895	81.3	68	37–40	10
9	G_9	1069	41.6	68	36–41	10
10	G_{10}	1054	28.4	68	41–42	10
11	G_{11}	874	21.6	68	1–2	10
12	G_{12}	954	14.2	68	2–3	10
13	G_{13}	948	43.3	68	3–5	10
14	G_{14}	595	46.8	68	4–3	10
15	G_{15}	588	27.9	56.8	8–9	10
16	G_{16}	744	95.701	68	10–11	10
17	G_{17}	744	119.715	68	12–13	10
18	G_{18}	892	4.9	80	45–44	10
19	G_{19}	1167	30.9	80	44–43	10
20	G_{20}	892	53.4	80	43–19	10
21	G_{21}	892	54.5	68	18–17	10
22	G_{22}	892	77	68	17–14	10
23	G_{23}	794	89	68	15–16	10
24	G_{24}	493	63.9	68	7–6	20
25	G_{25}	994	64.1	68	26–25	10
26	G_{26}	994	204.5	68	27–31	10
27	G_{27}	994	36.2	68	31–32	10
28	G_{28}	891	125.8	85	33–34	10
29	G_{29}	891	67.7	85	34–35	10
30	G_{30}	1000	0.001	68.7	20–19	10

Table 2 Pressure bound on pipeline nodes

Node	Pressure bounds	Node	Pressure bounds(bar)	Node	Pressure bounds(bar)
N_1	$40 \prec P \prec 49$	N_{15}	$40 \prec P \prec 68.7$	N_{29}	$40 \prec P \prec 68.7$
N_2	$40 \prec P \prec 68.7$	N_{16}	$40 \prec P \prec 68.7$	N_{30}	$40 \prec P \prec 67$
N_3	$40 \prec P \prec 68.7$	N_{17}	$40 \prec P \prec 68.7$	N_{31}	$40 \prec P \prec 68.7$
N_4	$40 \prec P \prec 68.7$	N_{18}	$40 \prec P \prec 68.7$	N_{36}	$40 \prec P \prec 68.7$
N_5	$40 \prec P \prec 68.7$	N_{19}	$40 \prec P \prec 68.7$	N_{37}	$40 \prec P \prec 68.7$
N_6	$40 \prec P \prec 68.7$	N_{20}	$40 \prec P \prec 68.7$	N_{38}	$60 \prec P \prec 86$
N_7	$40 \prec P \prec 49$	N_{21}	$40 \prec P \prec 68.7$	N_{39}	$P_{39} = 45$
N_8	$40 \prec P \prec 56.8$	N_{22}	$40 \prec P \prec 68.7$	N_{40}	$40 \prec P \prec 68.7$
N_9	$40 \prec P \prec 56.8$	N_{23}	$40 \prec P \prec 68.7$	N_{41}	$40 \prec P \prec 68.7$
N_{10}	$40 \prec P \prec 68.7$	N_{24}	$40 \prec P \prec 68.7$	N_{42}	$40 \prec P \prec 68.7$
N_{11}	$40 \prec P \prec 68.7$	N_{25}	$40 \prec P \prec 68.7$	N_{43}	$40 \prec P \prec 81$
N_{12}	$40 \prec P \prec 68.7$	N_{26}	$40 \prec P \prec 68.7$	N_{44}	$40 \prec P \prec 81$
N_{13}	$40 \prec P \prec 68.7$	N_{27}	$40 \prec P \prec 68.7$	N_{45}	$40 \prec P \prec 81$
N_{14}	$40 \prec P \prec 68.7$	N_{28}	$40 \prec P \prec 68.7$		

Table 3 Values of maximum supply and minimum fixed delivery rate (Tabkhi, 2007)

Description of gas supply nodes					
Gas source nodes	Gas injection rate	Node capacity (kg/s)	Gas source nodes	Notation for gas injection rate at the respective source station	Maximum gas supply capacity (kg/s)
N_1	ms_1	78.406	N_{30}	ms_{30}	474.331
N_4	ms_4	68.652	N_{39}	ms_{39}	400.564
N_{20}	ms_{20}	53.377	N_{45}	ms_{45}	90.786
Total gas supply capacity from all gas sources					1166.116
Description of gas delivery nodes					
Gas delivery nodes	Notation for gas rate throughput at the respective delivery station	Minimum gas delivery Rate (kg/s)	Gas Delivery Nodes	Notation for gas rate throughput at the respective delivery station	Minimum gas delivery Rate (kg/s)
N_2	m_{d_2}	75.678	N_{22}	$m_{d_{22}}$	59.507
N_3	m_{d_3}	146.964	N_{23}	$m_{d_{23}}$	16.15
N_5	m_{d_5}	36.824	N_{25}	$m_{d_{25}}$	63.628
N_6	m_{d_6}	42.596	N_{31}	$m_{d_{31}}$	0.393
N_9	m_{d_9}	23.011	N_{33}	$m_{d_{33}}$	6.866
N_{10}	$m_{d_{10}}$	19.987	N_{35}	$m_{d_{35}}$	172.76
N_{12}	$m_{d_{12}}$	20.436	N_{37}	$m_{d_{37}}$	62.274
N_{14}	$m_{d_{14}}$	41.693	N_{40}	$m_{d_{40}}$	126.622
N_{16}	$m_{d_{16}}$	42.064	N_{44}	$m_{d_{44}}$	73.574
N_{19}	$m_{d_{19}}$	119.988			
Total gas demand at all delivery stations					1151.015

Table 4 Bounds of compressors

Compressor	Notation for gas flow rate at the inlet of station	Upper bound for flow rate at inlet station to avoid choking (m^3/s)
C_1	q_{24}	156
C_2	q_{19}	486
C_3	q_{11}	208
C_4	q_5	267
C_5	q_{29}	667
C_6	q_{14}	378
C_7	q_{32}	264

the output strain. Table 1 shows the lower bounds for pressure at pipe nodes, Table 2 shows the lower and maximum gas supply, Table 3 shows the least amount of gas delivered, and Table 4 shows the maximum permissible gas flow rate to the individual compressor station.

Modeling equations

The following three sections demonstrate the gas pipeline modeling equations. The first section discusses the objective function equations used to reduce fuel expenditure in compressors and maximizes gas delivery at the distribution centers. The second section discusses the equations used to evaluate natural gas properties. Finally, in the third section, the pipeline and compressor modeling equations are presented.

Objective function

The first objective is to reduce fuel expenditure in compressor stations. Equation (1) depicts the fuel consumption in compressors. The second objective given in Eq. (2) is to maximize the gas delivery at the distribution centers (Arya & Honwad, 2018).

$$\begin{aligned}(O.F)_1 &= \min g(m_i, P_s, P_d)\\ &= \min \sum m_f\\ &= \sum_{i,j\in A_c}\left(\frac{m_j \times h_{ij}}{LHV_{NG}}\right)\times\left(\frac{10^6}{\eta_{is}\times\eta_{dr}\times\eta_{me}}\right)\end{aligned} \tag{1}$$

$$(O.F)_2 = \max(m_{de_{i=1-19}}) \tag{2}$$

Estimation of gas property

Natural gas property is estimated using Eqs. (3) to (7). Equation (3), Eq. (4) and (5), Eq. (6), and Eq. (7) calculate the average molecular weight of the gas mixture, critical

temperature and pressure of the gas, heat content of natural gas, and isentropic coefficient of gas, respectively (Mohring, 2004; Pambour et al. 2016).

$$M = \sum_{i=1}^{n} M_i \times y_i \tag{3}$$

$$T_C = \sum_{i=1}^{n} T_{Ci} \times y_i \tag{4}$$

$$P_C = \sum_{i=1}^{n} P_{Ci} \times y_i \tag{5}$$

$$H_m = \sum_{i=1}^{n} H_i \times y_i \times M_i \tag{6}$$

$$k = \frac{\sum_{i=1}^{n} C_{pi} \times y_i}{\sum_{i=1}^{n} C_{pi} \times y_i - R} \tag{7}$$

Pipeline modeling equations

This section presents the modeling equation developed for a pipeline grid system.

Gas flow equation Friction and elevation are the two significant factors for pressure loss in pipeline grids. Equation (8) is a general flow equation used for calculating pressure drop in cross-country gas pipelines. The equations consider both the elevation and friction losses occurring in the pipeline (Menon, 2005).

$$P_i^2 - e^s \times P_j^2 = \left(\frac{16 \times m_i^2 \times z_i \times R \times T}{\pi^2 \times D_i^4 \times M}\right) \left[\left(2 \times \log_{10}\left(\frac{P_i}{P_j}\right) - \left(\frac{f_i \times L_{ei}}{D_i}\right)\right)\right] \tag{8}$$

The pipeline is deemed horizontal; hence, Eq. (9) evaluates the gas pipeline pressure drop.

$$P_i^2 - P_j^2 = \left(\frac{16 \times m_i^2 \times z_i \times R \times T}{\pi^2 \times D_i^4 \times M}\right) \left[\left(2 \times \log_{10}\left(\frac{P_i}{P_j}\right) - \left(\frac{f_i \times L_i}{D_i}\right)\right)\right] \tag{9}$$

Friction factor equation The friction factor is a dimensionless parameter that accounts for energy losses between the gas and the pipeline wall. The American Gas Association (AGA), Colebrook's–White equation, and modified Colebrook equation calculate the friction factor. Among these equations, the Colebrook–White equation presented in Eq. (10) is the most recommended Equation for a fully rough and high Reynolds number in the pipeline (Menon, 2005).

$$f_i = -2 \log_{10}\left(\frac{e}{3.71 \times D_i}\right)^{-2} \tag{10}$$

The average pressure of the gas The pipeline's pressure varies as the gas moves from one section to another pipeline section. Hence, the average pressure value mentioned in Eq. (11) calculates the average gas pressure between two pipeline segments.

$$P_{ij} = \left(\frac{2}{3}\right) \times \left[P_i + P_j - \frac{P_i \times P_j}{P_i + P_j}\right] \tag{11}$$

Compressibility factor AGA, Standing-Katz, Dranchuk, CNGA methods are widely used to calculate the compressibility factor. The CNGA equation, because of its simplicity, is used in the present paper to calculate the compressibility factor (Menon, 2005; Tabkhi, 2008).

$$z_i = 1 + \left(0.257 - 0.533 \times \frac{T_{NG,C}}{T_g}\right) \times \frac{P_{ij}}{P_{NG,C}} \tag{12}$$

Gas velocity The pressure of the gas changes as it moves in the pipeline. The pressure is highest at the inlet station, while due to friction and elevation losses, it is lowest at the distribution centers. The gas's velocity is inversely proportional to pressure, and hence the speed is lowest at the inlet of pipe and highest at the outlet. Equation 13 measures the gas velocity in the pipeline (Menon, 2005).

$$v_i = 14.7359 \times \left(\frac{q_i \times 24 \times 3600}{\left(OD \times 10^3 - 2 \times t_i \times 10^3\right)^2}\right) \times \left(\frac{P_b}{T_b}\right) \times \left(\frac{z_i \times T_g}{P_{ij} \times 10^2}\right) \tag{13}$$

Compressor modeling equations

Isentropic head The compressor used in a pipeline receives gas at a specific pressure and then delivers the gas at elevated pressure after compression. The isentropic head, in

Eq. 14, is the energy added per unit mass of gas to increase the inlet to outlet pressure (Alinia et al. 2014).

$$h_{ij} = \left(\frac{z_i \times R \times T_g}{M_{NG}}\right) \times \left(\frac{k}{k-1}\right) \times \left[\left(\frac{P_j}{P_i}\right)^{\frac{k-1}{k}} - 1\right] \tag{14}$$

Isentropic efficiency Isentropic efficiency measures the compressor's current output to its theoretical performance at the identical entrance and outlet conditions. The equation, shown in Eq. (15), measures the overall isentropic performance of compressors (Smith and Van Ness, 1998).

$$\eta_{is} = \frac{\left(\frac{P_d}{P_s}\right)^{\frac{\gamma-1}{\gamma}} - 1}{\left(\frac{P_d}{P_s}\right)^{\frac{n_p-1}{n_p}} - 1} \tag{15}$$

Constraints on Gas pipeline grid and compressors

The objective functions reported in Eqs. 1 and 2 involve a multi-objective function, which requires different inequalities and equality restrictions to be satisfied. Equations 16–28 are the inequality and equality constraints imposed on the gas pipeline grid.

Erosional velocity In the pipeline, the gas velocity should be kept as high as possible but not above the value obtained from the erosional velocity given in Eq. (16). Keeping the velocity higher than the erosional velocity leads to erosion, vibration, and noise in the pipeline (Menon, 2005).

$$v_{ei} \le 122\sqrt{\frac{z_i \times R \times T_g}{P_{ij} \times M_{NG}}} \tag{16}$$

Table 5 Gas consumed(kg/s) at compressor station using Tabkhi (2008) and Arya (2018) Model

S. No	Compressor no	Tabkhi model	Arya model
1	Compressor 1	0	0
2	Compressor 2	0	0
3	Compressor 3	0	0
4	Compressor 4	0	0
5	Compressor 5	0.05	0.052
6	Compressor 6	0	0
7	Compressor 7	0.320	0.321
	Total Fuel Consumed(kg/s)	0.74	0.746

Maximum allowable operating pressure (MAOP) The pressure should be kept as high as possible in the pipeline (Menon, 2005). However, the pressure should not go beyond the pressure value obtained from Eq. (17) for safety consideration (Table 5).

$$(MAOP) = \frac{2 * t_i * S * E * F * T}{(OD)_i} \tag{17}$$

Choking of pipeline Equation (18) limits the flow rate of gas to avoid choking in compressors (Gorla and Khan, 2003)

$$q_{i\max} \prec \left(\frac{\pi}{4} \times D_i^2\right) \times \left(\sqrt{\frac{\gamma \times z_i \times R \times T_g}{M_{NG}}}\right) \times \left(\frac{2}{\gamma+1}\right)^{\frac{\gamma+1}{2\times(\gamma-1)}} \tag{18}$$

Mass balance equations The mass conservation principle states that 'mass is neither created nor destroyed.' The same principle governs each pipe node. Equation (19) is the general mass balance equation further simplified to Eq. (20).

$$\lim_{\Delta t \to 0}\left(\frac{\begin{pmatrix} mass\ at \\ t+\Delta t \end{pmatrix} - \begin{pmatrix} mass\ at \\ time\ t \end{pmatrix}}{\Delta t}\right)$$
$$= \lim_{\Delta t \to 0}\left(\frac{\begin{matrix} Mass\ entering\ to\ node \\ from\ time\ t\ to\ t+\Delta t \end{matrix}}{\Delta t} - \frac{\begin{pmatrix} Mass\ exiting\ from \\ node\ time\ t+\Delta t \end{pmatrix}}{\Delta t}\right)$$
$$+ \lim_{\Delta t \to 0}\left(\frac{\begin{pmatrix} net\ chemical\ production \\ between\ t\ and\ t+\Delta t \end{pmatrix}}{\Delta t}\right) \tag{19}$$

$$\begin{pmatrix} mass\ accumulation \\ rate \end{pmatrix} = \begin{pmatrix} mass\ flux \\ in \end{pmatrix} - \begin{pmatrix} mass\ flux \\ out \end{pmatrix} + \begin{pmatrix} net\ rate \\ of\ production \end{pmatrix}$$

$$\frac{dm}{dt} = m_{in} - m_{out} \tag{20}$$

Equations 21–28 are the mass balance equations applied to various nodes of the pipeline grid. Table 6 reports these mass balance equations.

Table 6 Mass balance on pipe nodes

Node	Mass balance eqn	Equation no	Node	Mass balance eqn	
N_{25}	$m_1 + m_{25} = m_{de_{25}} + m_2$	21	N_{27}	$V_3 + V_4 + m_{26} + m_{f_5} = m_6$	40
C_1	$m_3 + m_{f_1} + m_{de_{23}} = m_2$	22	N_{31}	$m_{27} + m_{de_{31}} = m_{26}$	41
N_{22}	$m_4 + m_{de_{22}} = m_3$	23	C_3	$m_{16} = m_{f_3} + m_{de_{12}} + m_{17}$	42
N_{19}	$m_{20} + m_{30} + V_7 = m_{de_{19}} + m_{f_2} + m_{21}$	24	V_1	$m_{15} = V_1$	43
N_{44}	$m_{18} + m_{de_{44}} = m_{19}$	25	N_{10}	$m_{16} + m_{de_{10}} = V_9$	44
N_{43}	$m_{19} = m_{20}$	26	N_1	$m_{11} = m_{s_1}$	45
N_{17}	$m_{22} = m_{21} + V_2$	27	N_{30}	$m_6 = m_{s_{30}}$	46
N_{14}	$m_{22} = m_{23} + V_8 + m_{de_{14}} + m_{f_6}$	28	N_{20}	$m_{30} = m_{s_{20}}$	47
N_3	$m_{13} + m_{de_{23}} = m_{12} + m_{14}$	29	N_{45}	$m_{18} = m_{s_{45}}$	48
N_2	$m_{12} + m_{de_2} = m_{11} + V_5$	30	N_{39}	$m_5 = m_{s_{39}}$	49
N_{34}	$m_{28} = m_{29}$	31	N_{36}	$m_7 + V_{10} = m_9$	50
N_{35}	$m_{29} = m_{de_{35}}$	32	N_{28}	$m_7 = V_3$	51
N_{33}	$m_{27} + V_2 = m_{f_7} + m_{de_{33}} + m_{28}$	33	N_{26}	$V_4 = m_1 + m_{25}$	52
N_{37}	$V_6 = m_{de_{37}} + m_8 + V_{10}$	34	N_{42}	$m_{10} = V_5$	53
N_{40}	$m_8 = m_{de_{40}}$	35	N_{38}	$m_5 = V_6$	54
N_5	$m_{24} + m_{de_5} + m_{f_4} + V_1 + V_9 = m_{13}$	36	N21	$V_7 = m_4$	55
N_6	$m_{24} = m_{de_6}$	37	N17	$V_2 + m_{21} = m_{22}$	56
N_9	$m_{15} = m_{de_9}$	38	N_{13}	$V_8 = m_{17}$	57
N_{16}	$m_{23} = m_{de_{16}}$	39	Overall	$m_s = m_{de} + m_f$	58

Multi-objective Ant colony optimization

The technique has its roots that mimic the foraging behavior of 'natural ants.' Ant communities such as 'Linepithema Humile' have a natural ability to lay down chemical pheromones when they move from the origin to their hives. Pheromones attract more ants to the same food supply. The pheromelia laid by the ants continue to dissipate; thus, the easier and quicker pathway has a stylistic fixation over the longer routes. The stigmergy attracts numerous ants to pick up the more straightforward path. This conduct of ants has been a *critical* source for ant colony algorithm's development initially by Dorigo, 1992. Different specialists later investigated the essential idea of insect state streamlining method to make counterfeit ants that likewise take care of the genuine enhancement issues (Schlueter, 2012; Socha and Blum, 2006; Maniezzo et al. 1994, Iredi et al. 2001; Stutzle and Hoos, 2000). The current practice revolves around one of these techniques (Schlueter, 2012). We've explored the method's crucial steps further in greater detail.

Step I Transform the bi-objective issue into a single factual issue.

Step II Develop the framework for the solution matrix.

Step III Matrix initialization with random solutions.

Step IV Stochastically search for a refined solution.

Step V Solution update.

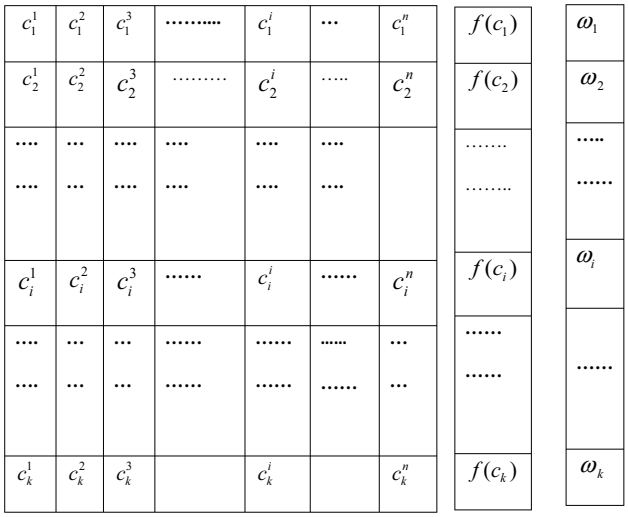

Fig. 2 Solution Matrix created by MOACO. The solutions are to be kept in the order of their Weights ($\omega_1 \geq \omega_2 \geq ...\omega_i \geq ....\omega_i$), from top to bottom

Step I Transform the bi-objective issue into a single factual issue A dilemma with many objectives is resolved using an adaptive strategy. Equation (21) shows the methodology of converting a multi-objective goal to a single objective one.

$$F_{MO} = (w_{f-1}) \times F_{MO}^{f-1} + (1 - w_{f-1}) \times F_f \tag{21}$$

Here $F_{MO}^1 = F_1$.

In our case, it was a bi-objective problem; hence Eq. (22) was used:

$$F_{MO} = (w_1) \times F_1 + (1 - w_1) \times F_2 \tag{22}$$

Step II Develop the framework for solution matrix

While hunting for food, ants carefully record the routes they have explored to return to their hive. In the process, they lay pheromone that serves as a guideline for other ants to find the same food. The solution matrix is generated similarly. Initially, the solution is found and stored in the matrix at random. This solution 'm' matrix serves as a guideline to further improve the solution. Figure 2 illustrates a general MOACO matrix. The matrix considers the 'n' number of variables in the 'k's number of objectives.

Step III Matrix initialization with random solutions

In the MOACO method, an initial guess for the 'n' variables and the 'k's number of objectives initializes the solution matrix. In each step, MOACO gives rise to the 'l' number of goals. After which 'k' options are retained from 'k + 1'in the search space, the remaining rejected.

Step IV Stochastically search for a refined solution

To initialize the matrix, it must create a random set of variables that result in many possible solutions. A probabilistic function P(x), referred to as Gaussian probability distribution, given in Eq. (23), is used to find the set of solutions from the second step onwards.

$$P^i(x) = \sum_{l=1}^{k} w_l p_l^i(x) = \sum_{l=1}^{k} w_l \left(\frac{1}{\sigma_l^i \sqrt{2\pi}} \right) \exp\left(\frac{-\left(x - \mu_l^i\right)^2}{2\sigma_l^{i^2}} \right) \tag{23}$$

The solution weight (w), means of solution (μ) and the standard deviation (σ) are the three parameters used in Eq. (23) that help the MOACO to generate new solutions.

Equation (24) calculates the solution weight. It corresponds to the solution's attractiveness based on minimizing or maximizing the solution to be carried in the next iteration.

$$w_j = \frac{1}{qk\sqrt{2\pi}} \exp\left(\frac{-(rank(j) - 1)^2}{2q^2k^2} \right) \tag{24}$$

The mean $rank(j)$ is derived by setting the Gaussian probability function equal to 1. q and k are the parameters used in MOACO. The weight 'w' facilitates finding the appropriateness of the procedure. Equation (25) utilizes the weight w to find the probability of a solution being carried forward in the next generation.

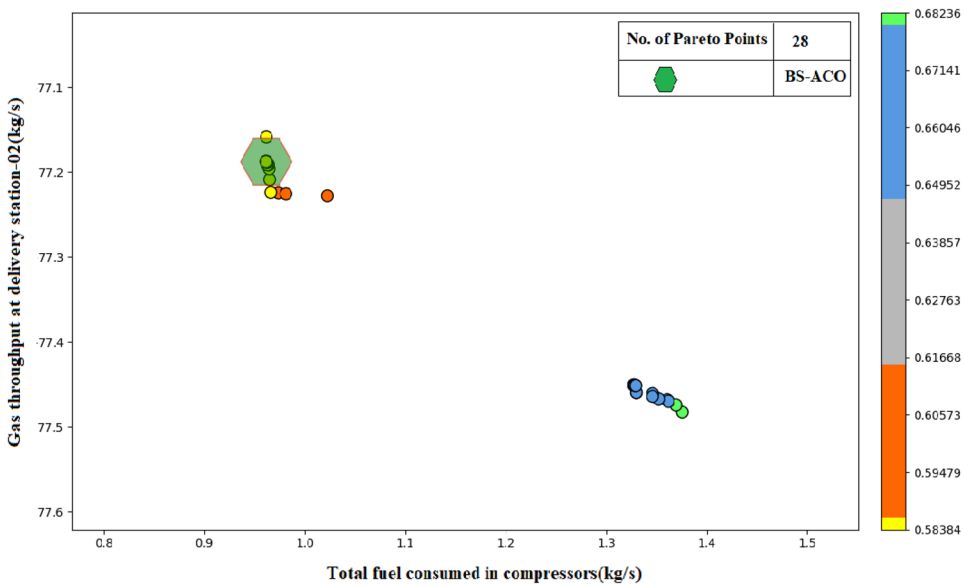

Fig. 3 Pareto front for fuel consumption versus throughput at delivery station—02

Table 7 Best throughput and corresponding fuel consumption obtained using MOACO

Delivery station →	02	03	05	06	09	10	12	14	16	19	22
Best throughput using MOACO →	77.18	141.32	36.89	44.13	19.94	20.23	29.12	47.36	38.61	122.00	48.67
Compressor no	Gas consumed in compressor stations										
C1	0.068	0.047	0.06734	0.037	0.030	0	0.077	0.008	6.3E-07	0.073	0
C2	0	0	0	0	0	0	0	0	5E-07	0	0
C3	0.027	0.033	0.046	0.048	0.021	0	0.014	0.026	0.002	0.020	0.013
C4	0.04	0.034	0.087	0.098	0.078	0.004	0.057	0.066	0.022	0.031	0.0317
C5	0.485	0.493	0.526	0.563	0.446	0.127	0.431	0.164	0.271	0.196	0.367
C6	0	0	0	0	0	0	0	0	6.9E-08	0	0
C7	0.34	0.371	0.350	0.375	0.415	0.320	0.268	0.323	0.2421	0.411	0.351
Total fuel consumed	0.96	0.980	1.078	1.123	0.992	0.452	0.850	0.588	0.539	0.733	0.763
No of pareto points	28	45	13	28	40	36	7	23	97	5	51

Delivery station →	23	25	31	33	35	37	40	44
Best throughput using MOACO →	14.64	20.22	10.64	4.07	167.00	45.94	126.22	68.58
Compressor no	Gas consumed in compressor stations							
C1	0.054	0	0	0.048	0.074	0.048	0.007	0.035
C2	1.137E-05	0	1.5E-07	0	0	0	0	0
C3	2.8543E-05	0	6.7E-07	0.018	0.022	0.004	0	0
C4	0.018	0.004	0.035	0.014	0.017	0.014	0.016	0.029
C5	1.7447E-05	0.127	0.110	0.140	0	0	0	0
C6	0	0	8.3E-09	0	0	0	0	0
C7	0.281	0.320	0.339	0.206	0.270	0.171	0.332	0.285
Total fuel consumed	0.353	0.452	0.485	0.428	0.385	0.238	0.357	0.350
No of pareto points	58	36	42	30	20	70	42	45

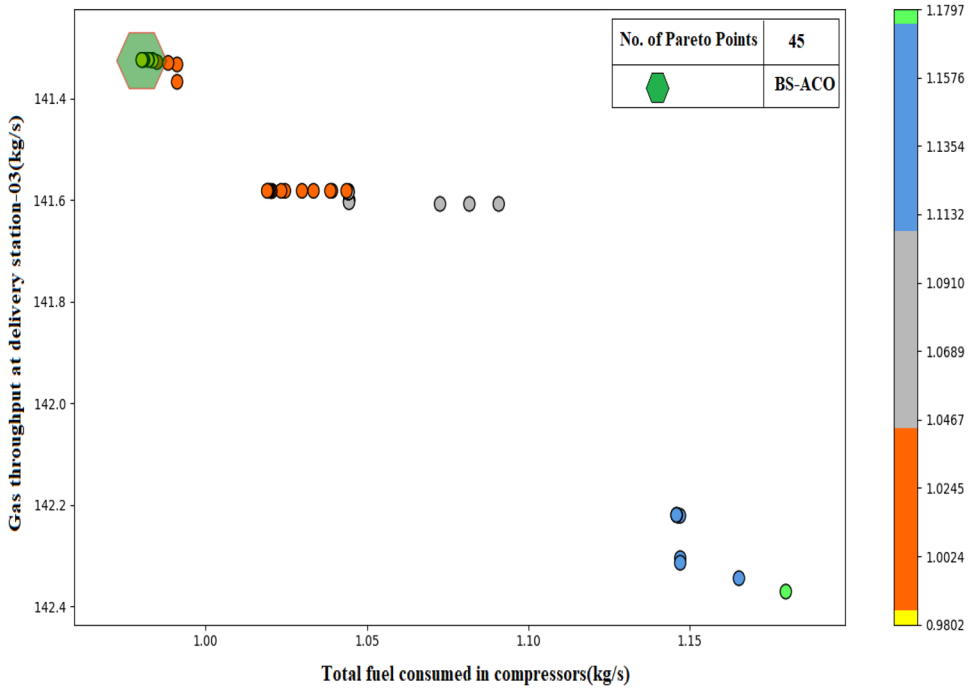

Fig. 4 Pareto front for fuel consumption versus throughput at delivery station—03

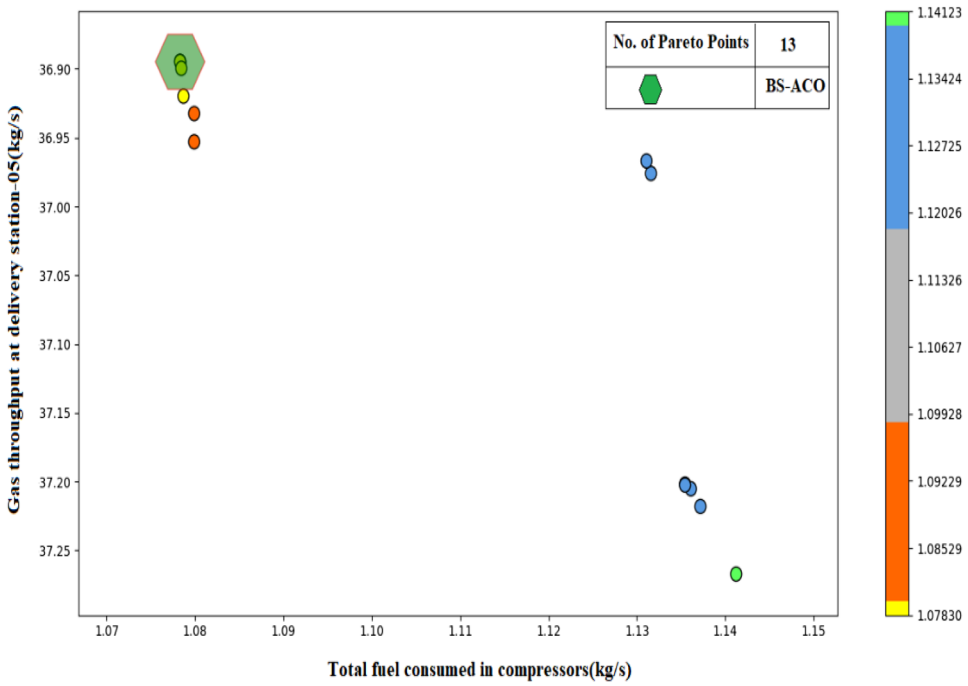

Fig. 5 Pareto front for fuel consumption versus throughput at delivery station—05

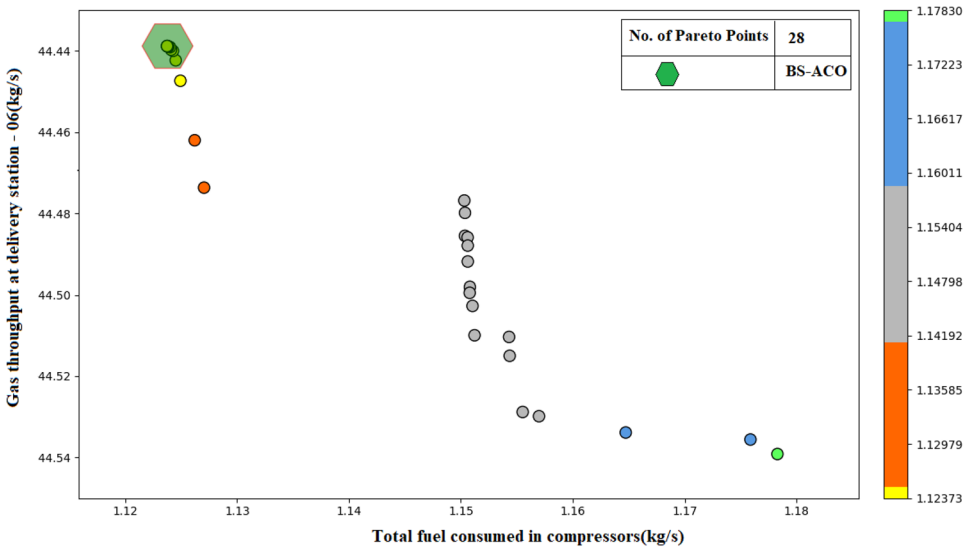

Fig. 6 Pareto front for fuel consumption versus throughput at delivery station—06

$$p_j = \frac{w_j}{\sum_{l=1}^{k} w_l} \tag{25}$$

The mean of the solution μ and the standard deviation σ is calculated from Eqs. (26) and (27).

$$\mu_l^i = c_l^i \tag{26}$$

$$\sigma = \xi \sum_{l=1}^{k} \frac{\left| d_l^i - d_j^i \right|}{k-1} \tag{27}$$

The term d_l^i and d_j^i are the two solutions in the solution matrix. 'ξ' Is a factor that allocates the convergence speed to the solution. A lower value ξ is given for a higher rate of convergence.

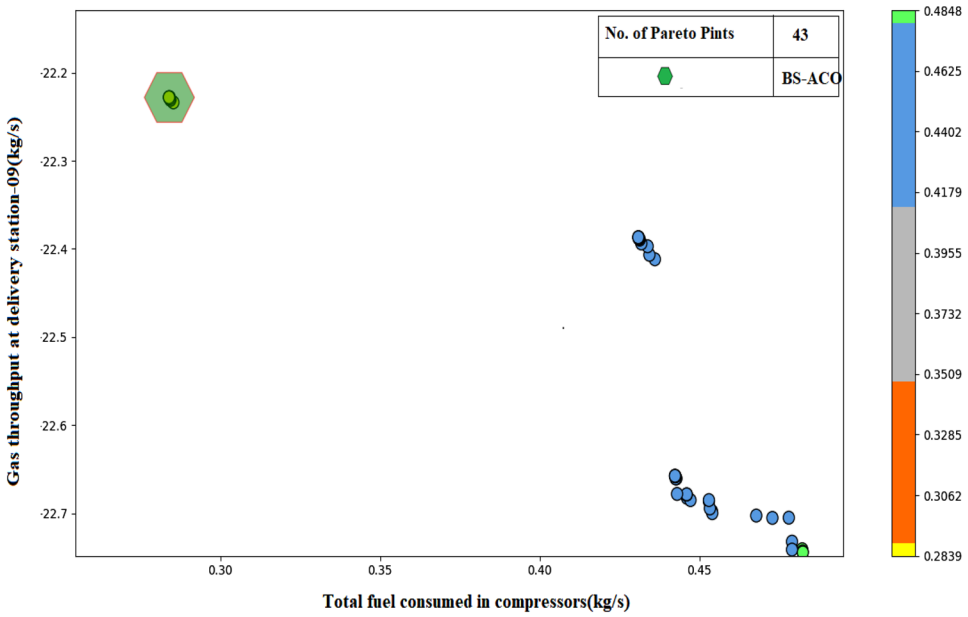

Fig. 7 Pareto front for fuel consumption versus throughput at delivery station—09

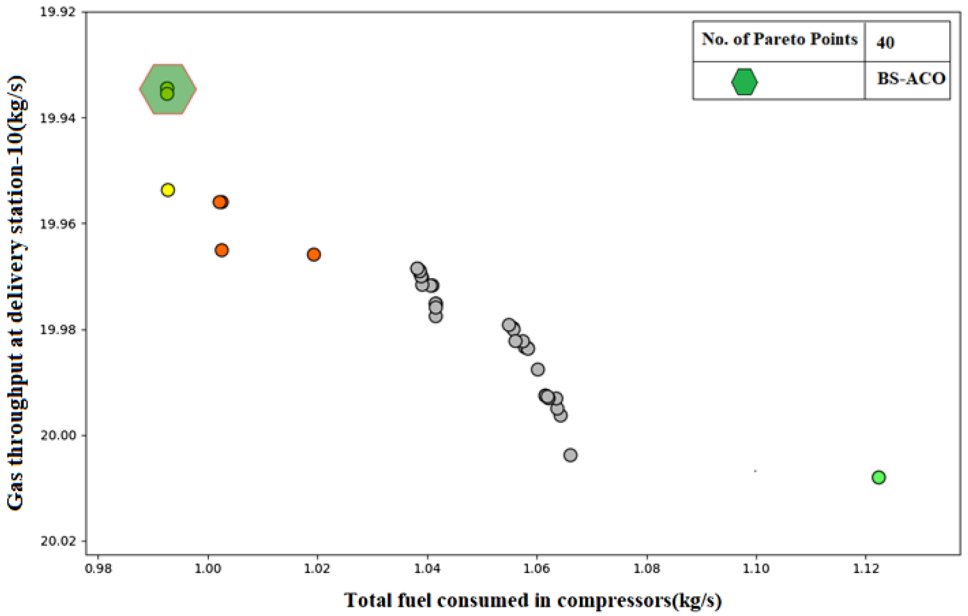

Fig. 8 Pareto front for fuel consumption versus throughput at delivery station—10

Step V Solution update

The three parameters, weight, mean, and standard deviation, update each iteration's solution matrix.

Model and optimization technique Validation

Previously the model was validated for the multi-distribution pipeline grid (Arya, 2018a). Table 5 highlights the key findings. The MOACO technique was validated for gun barrel paper (Arya, 2018b). Despite having several advantages, the technique has not been used in a multi-distribution pipeline. The paper explores the benefit of implementing the MOACO technique in a multi-distribution pipeline grid system. Two stopping criteria are applied to the MOACO optimization program. The first stopping criterion chosen is the stopping time of the optimization process, which was kept as 2000s. The second stopping criterion used was the maximum number of evaluations that are kept as 10 million. The second stopping criterion ensures that the optimization search is carried out until 10 million function evaluations do not improve the current solution.

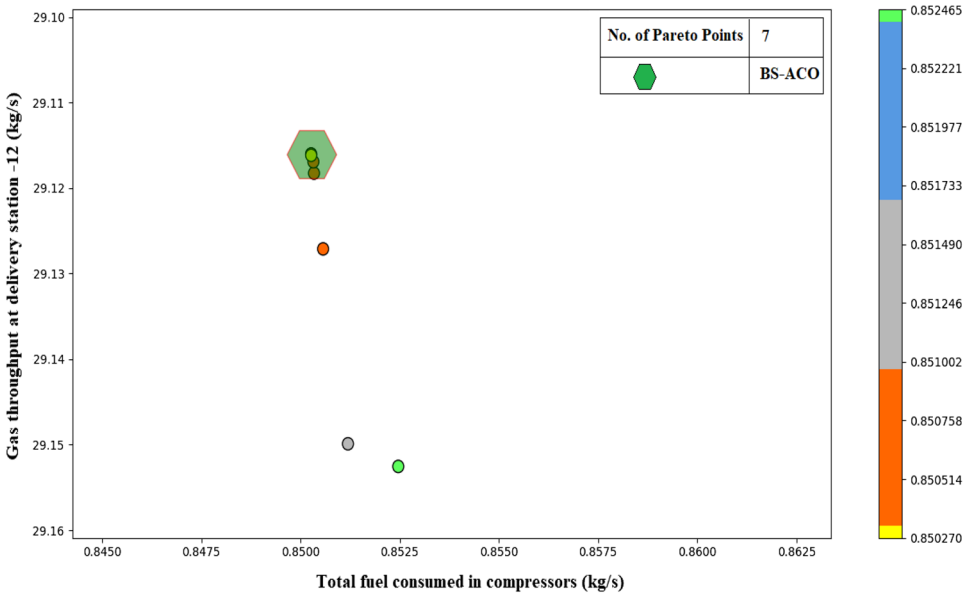

Fig. 9 Pareto front for fuel consumption versus throughput at delivery station—12

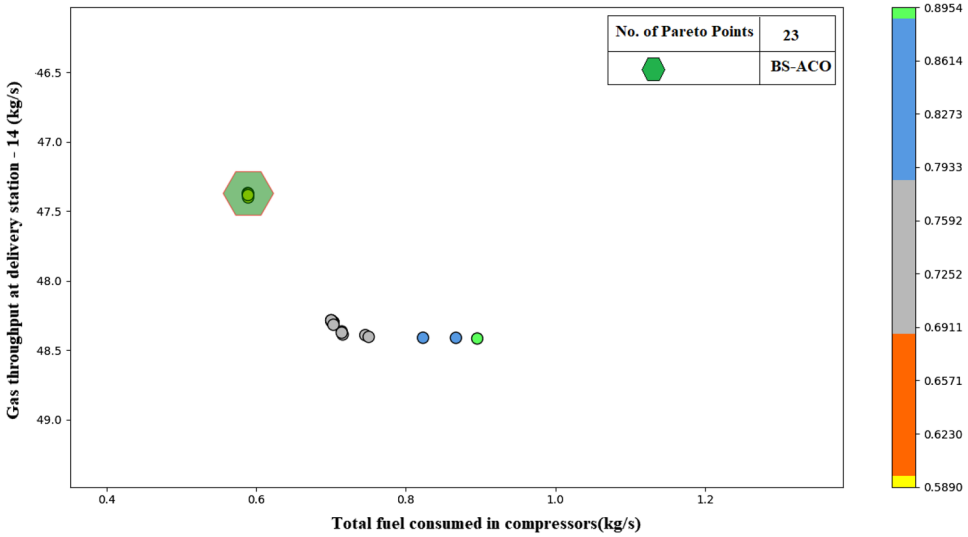

Fig. 10 Pareto front for fuel consumption versus throughput at delivery station—14

Result and discussion

The pipeline grid considered for the study is depicted in Fig. 1. "Pipeline grid description" section discusses the network in depth. Ninety-nine variables comprise the pipeline grid. These include forty-five pressure variables, thirty gas flow rate variables, seven fuel consumption in compressors, six gas supply, and ten valve flow rate variables. The network consists of nineteen delivery points. One gas delivery parameter is retained as a variable to determine the maximum amount of gas supplied at that particular distribution node. These calculations are performed on an individual basis for each distribution node. The multi-objective optimization applied to each distribution node facilitates the pipeline operator to deal the situations such as forecast error in gas requirement at delivery stations, inconsistent gas consumption in compressors and change in ambient temperature. The conditions lead to variations in gas requirements at different delivery nodes. The multi-objective plot will help the operators analyze the gas delivered at different delivery stations and the corresponding fuel consumption. Running the optimizer at the various nodes also informs the optimum gas amount delivered at the delivery stations. Table 2 details the bare minimum amount of gas distribution that must be guaranteed. The multi-objective ant colony technique is applied to the nineteen gas distribution points, and the Pareto points are generated for each delivery point. The delivery station (02) is the first delivery point chosen on which the MOACO is implemented. The Pareto front was created to

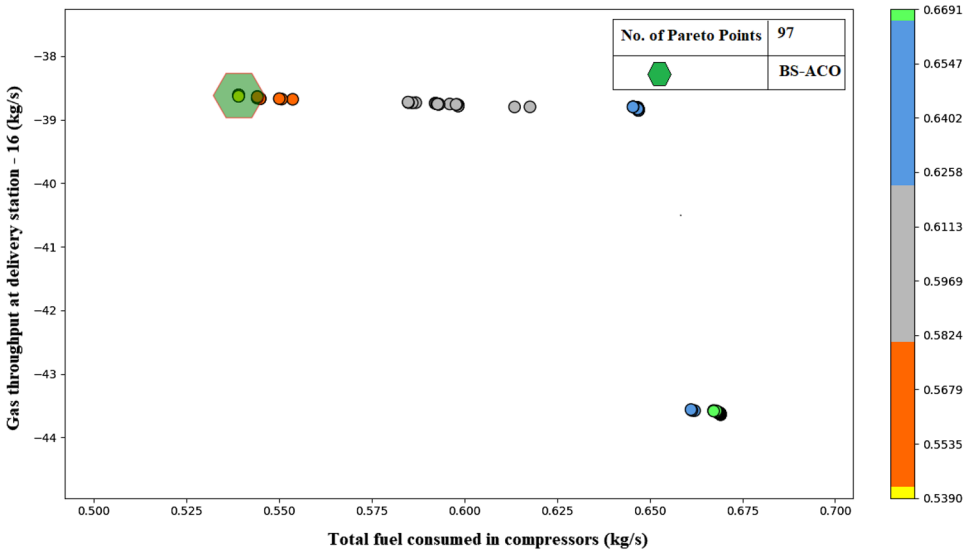

Fig. 11 Pareto front for fuel consumption versus throughput at delivery station—16

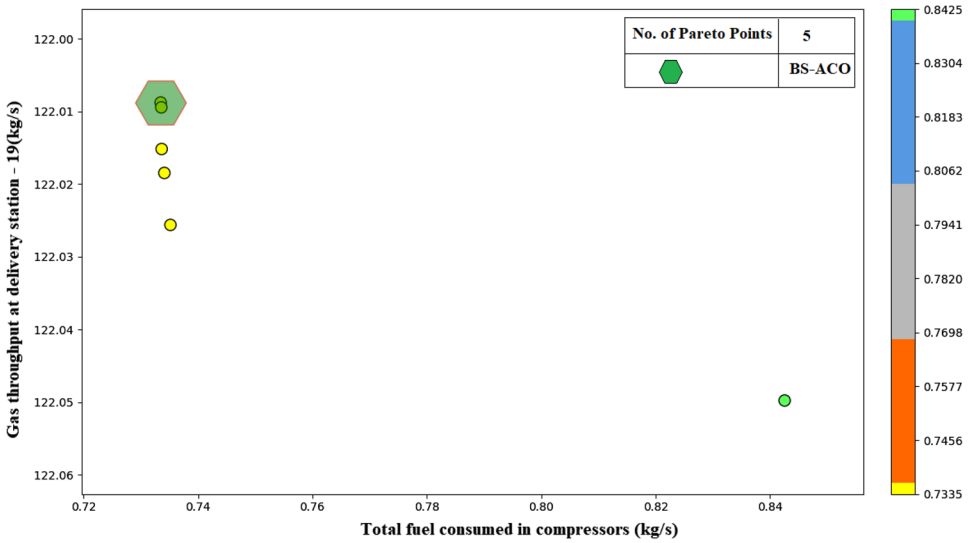

Fig. 12 Pareto front for fuel consumption versus throughput at delivery station—19

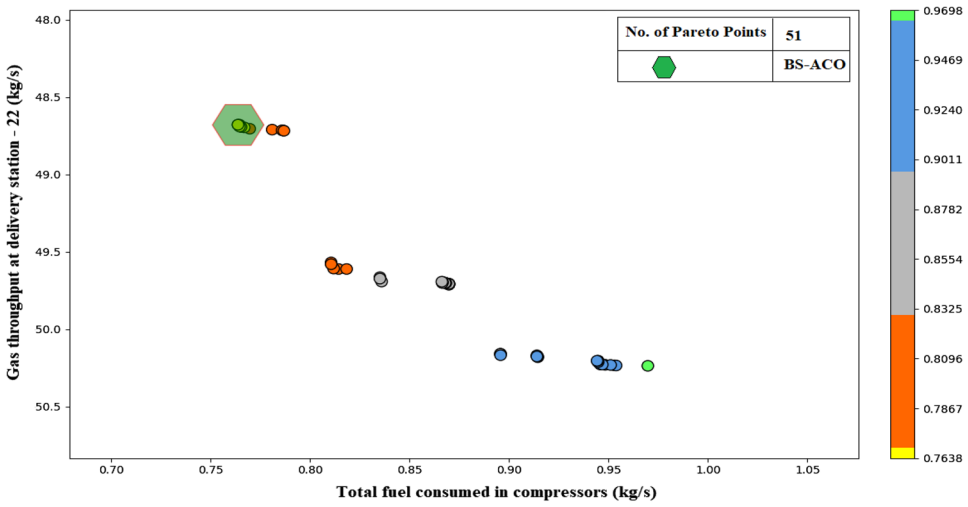

Fig. 13 Pareto front for fuel consumption versus throughput at delivery station—22

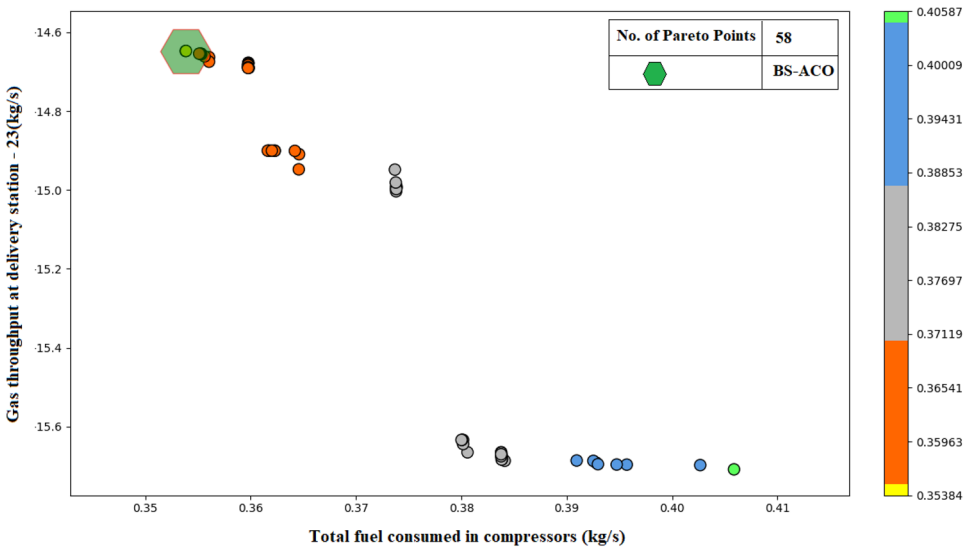

Fig. 14 Pareto front for fuel consumption versus throughput at delivery station—23

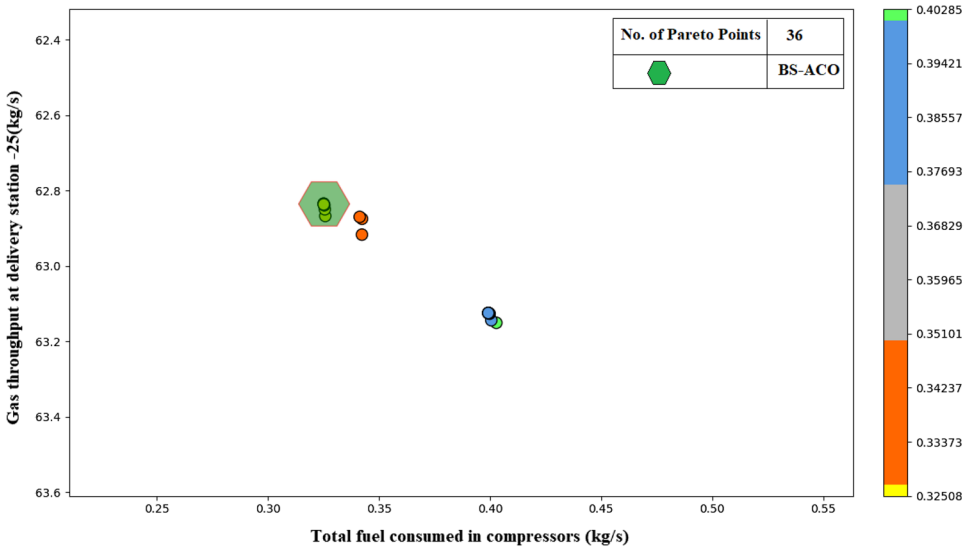

Fig. 15 Pareto front for fuel consumption versus throughput at delivery station—25

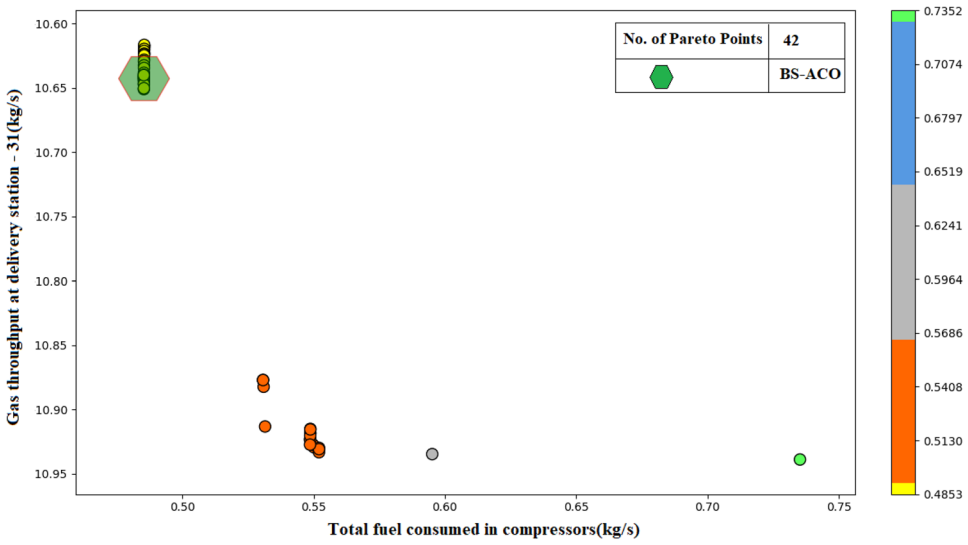

Fig. 16 Pareto front for fuel consumption versus throughput at delivery station—31

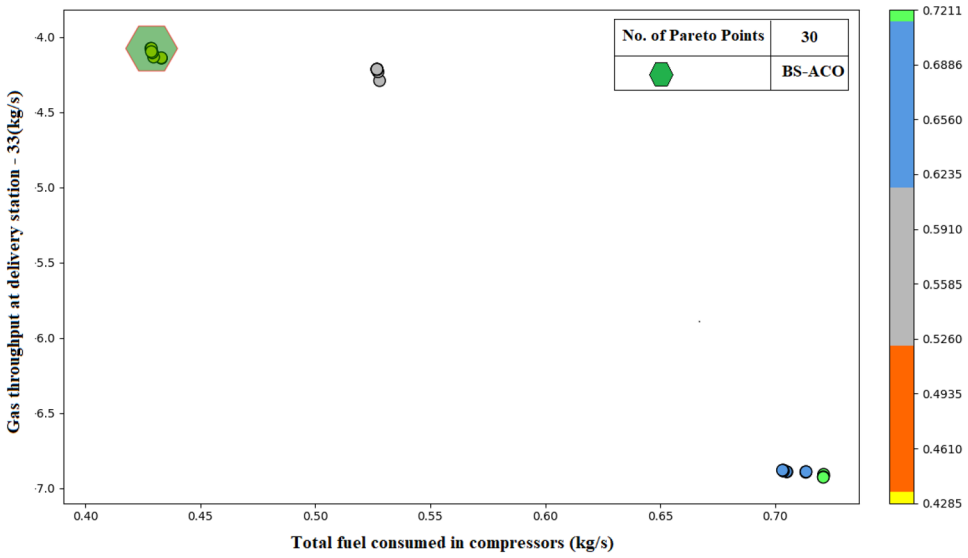

Fig. 17 Pareto front for fuel consumption versus throughput at delivery station—33

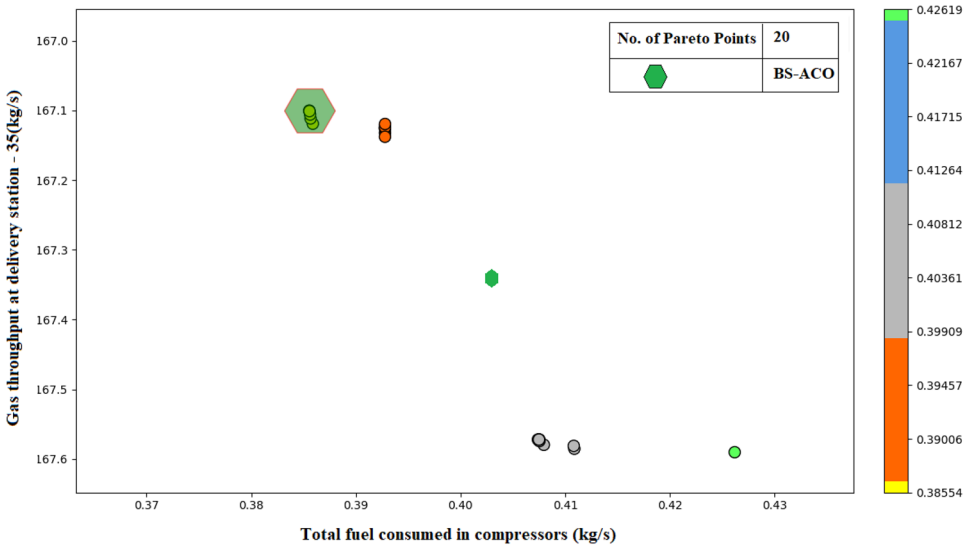

Fig. 18 Pareto front for fuel consumption versus throughput at delivery station—35

keep fuel usage to a minimum and obtain the greatest possible throughput at the distribution station(02). The Pareto front generated gives a set of twenty-eight Pareto points. The Pareto front gives critical information that one objective on a Pareto front cannot be improved without worsening the second objective function. A similar scenario is seen in the Pareto front, shown in Fig. 3. As we progress on the Pareto front, fuel usage increases (worsening the second objective function). The criterion satisfies the Pareto front's characteristics and shows that the Pareto front obtained for the distribution station is correct. The figure also shows that the maximum amount of gas delivered at this station is 77.18 kg/sec. The corresponding fuel consumed is 0.96 kg per second. The amount of gas consumed in individual gas compressors corresponding to the delivery station (02) is discussed in Table 7.

Further, the Pareto front obtained in Fig. 4 for gas distribution at the delivery station (03) shows that the maximum amount of gas sent at the delivery station (03) is 141.32 kg per second. The corresponding gas consumed at the seven compressors is 0.980 kg per second. A similar Pareto is obtained for each of the nineteen gas distribution stations. The Pareto front drawn Pareto front for each distribution point is shown in Fig. 3–21. Figure 5 shows the maximum gas delivery at distribution point (05) is 36.89 kg per second, and the corresponding fuel consumption is 1.078 kg per second. A total of 13 Pareto points are obtained. Figure 6 shows the Pareto front for the gas delivery at the delivery station (**06**) and the corresponding fuel consumption. The maximum delivery achieved is 44.13 kg per second, and the corresponding fuel consumption is 1.123 kg per second. Figure 7 shows the Pareto front at

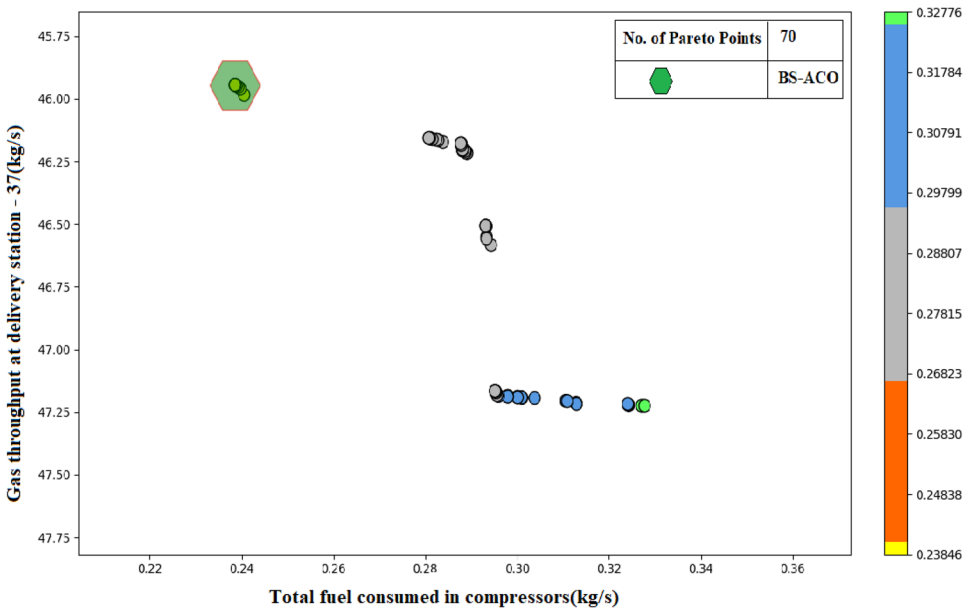

Fig. 19 Pareto front for fuel consumption versus throughput at delivery station—37

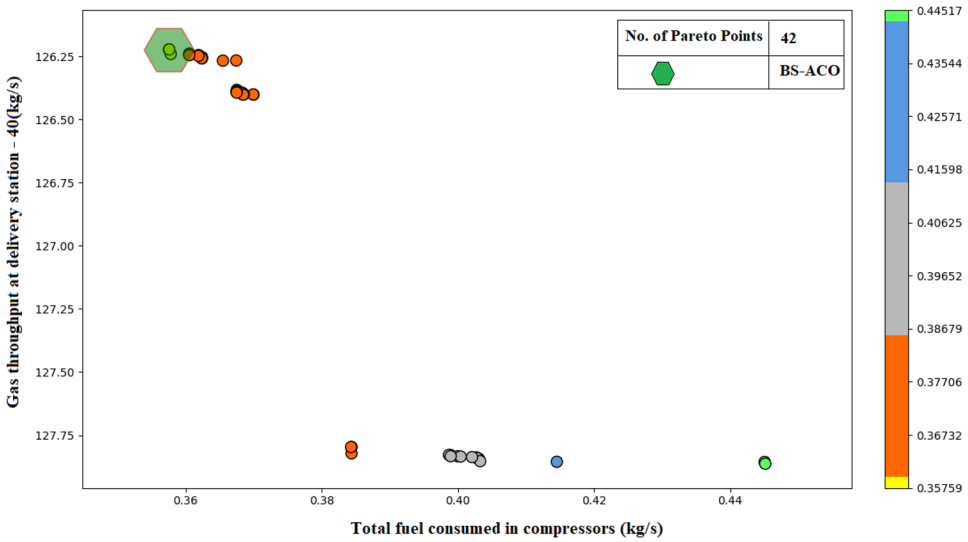

Fig. 20 Pareto front for fuel consumption versus throughput at delivery station—40

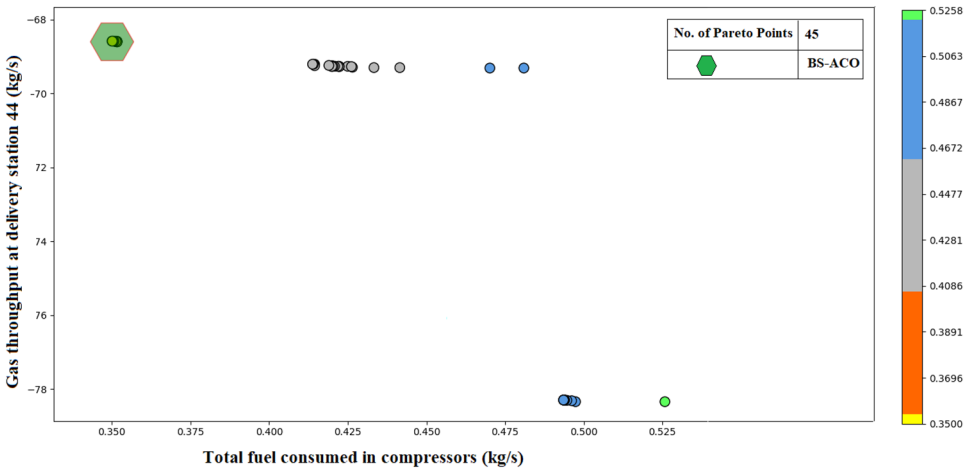

Fig. 21 Pareto front for fuel consumption versus throughput at delivery station—44

the distribution center (09). Figure 8 shows the Pareto front for the delivery station (10), Fig. 9 for the delivery station (12), Fig. 10 for the delivery station (14), Fig. 11 for the delivery station (16), Fig. 12 for the delivery station (19), Fig. 13 for the delivery station (22), Fig. 14 for the delivery station (23), Fig. 15 for the delivery station (25), Fig. 16 for the delivery station (31), Fig. 17 for the delivery station (33), Fig. 18 for the delivery station (35), Fig. 19 for the delivery station (37), Fig. 20 for the delivery station (40), and Fig. 21 for the delivery station (44). It is crucial to note that improving one objective worsens the second objective function for each Pareo front obtained for the corresponding distribution station. Figures 3–21 show that all the Pareto points obtained for individual distribution stations are equally good. In figures like Figs. 4, 6 and 9, not much variation is seen in gas throughput along the Pareto point curve. The effect shows that the best operating points are obtained when the pipeline is run at almost full capacity. Table 7 shows the best solutions for the highest delivery at each distribution station and the corresponding fuel consumption in compressors.

Conclusion

The article provides a statistical model for multi-distribution gas grids. Ant colony optimization technique is implemented on the proposed model. The optimization strategy optimizes the multi-objective role of limiting the fuel consumption in compressors and maximizing the gas pipeline grid's throughput at nineteen distribution stations. Both the goals are balanced by choosing optimal pressure at forty-five pipe nodes and gas flow rate in thirty pipe legs. MOACO was implemented to a 30-pipe arc pipeline grid to build Pareto optimal multi-objective solutions. A multi-objective approach to the gas pipeline grid issue tends to achieve numerous solutions, from which decision-makers can select the most suitable one based on a conversation with a manager. The optimal results produced for multi-objective optimization advocate the industrial method of reducing fuel usage at the cost of the low performance of the gas throughput of the system. The methodology may develop techniques for enhancing a gas pipeline grid's operational conditions and performance.

Funding No funding was received.

Declarations

Conflict of interest The authors declared that they have no conflict of interest.

References

Adeyanju OA, Oyekunle LO (2004)Optimization of natural gas transportation in pipelines. Petroleum and gas engineering program. Nigeria: Univ. of Logos.

Alves F, da Silva J, Miranda N (2016) Multi-objective design optimization of natural gas transmission networks. Comput Chem Eng 93:212–220

Arya AK, Honwad S (2015) Modeling, simulation and optimization of a high-pressure cross-country natural gas pipeline: application of ant colony optimization technique. J Pipeline Syst Eng Pract. 7

Arya AK, Honwad S (2018) Optimal operation of a multi-source multi-delivery natural gas transmission pipeline network. Chem Prod Process Model 13:1–17

Arya AK, Honwad S (2018) Multi-objective optimization of a gas pipeline network: an ant colony approach. J Petrol Explor Prod Technol 8:1389–1400

B.P (2013) Statistical review of world energy. technical report british petroleum (B.P.), London

Boyd ID, Slurry PD, Radcliffe NJ (1994) Constraint gas network pipe sizing with genetic algorithm. Edinburgh Parallel computing center, Technical Report EPCC-TR94–11

Carter RG (1996) Compressor station optimization: computational accuracy and speed. 28th Annual Meeting of Pipeline Simulation Interest Group, San Francisco, C.A

Carter RG (1998) Pipeline optimization: dynamic programming after 30 years," in PSIG Annual Meeting, PSIG, Denver, USA

Chebouba A (2015) Multi objective optimization of line pack management of gas pipeline system. InJournal of Physics: Conference Series 2015 Jan 21 (Vol. 574, No. 1, p. 012114). IOP Publishing

Demissie A, Zhu W, Belachew CT (2017) A Multi-objective optimization model for gas pipeline operations. Comput Chem Eng 100:94–103

Demissie A, Zhu W (2015) "A survey on gas pipelines operation and design optimization keywords :" In *A Survey on Gas Pipelines Operation and Design Optimization*. 734–43

Dorigo M (1992) Optimization, learning and natural algorithms. Ph.D. Thesis, Italy: Politecnico di Milano

Edger TF, Himmelblau DM (2001) Optimization of chemical processes. McGraw Hill, Singapore

Elbeltagi E, Hegazy T, Grierson D (2005) Comparison among five evolutionary-based optimization algorithm. Adv Eng Inform 19(1):43–53

Fasihizadeh M, Sefti MV, Torbati HM (2014) Improving gas transmission networks operation using simulation algorithms: case study of the national iranian gas network. J Nat Gas Sci Eng 20:319–327

Fodstad M, Midthun KT, Tomasgard A (2015) Adding flexibility in a natural gas transportation network using interruptible transportation services. Eur J Oper Res 43(2):647–657

Goldberg DE, Kuo CH (1985) Genetic algorithms in pipeline optimization. In: Pipeline Simulation Interest Group, Annual Meeting. October 24–25, Albuquerque, New Mexico

Gorla RSR, Khan AA (2003) Turbomachinery design and theory, Marcel Dekker Inc. New York, USA

Guerra OJ, Calderón AJ, Papageorgiou LG, Siirola JJ, Reklaitis GV (2016) An optimization framework for the integration of water management and shale gas supply chain design. Comput Chem Eng 92:230–255

Guo B, Ghalambor A (2005) Natural gas engineering handbook, 1st edn. Gulf Publishing Company, Houston, Texas

Hamedi M, Farahani RZ, Esmaeilian G (2011) Optimization in Natural gas network planning.". Log Oper Manag. https://doi.org/10.1016/B978-0-12-385202-1.00019-0

Hawryluk AKK, Botros GH, Huynh B (2010) Multi-objective optimization of natural gas compression power train with genetic algorithms. Presented at the 8th International Pipeline Conference, Volume 3, Calgary, IPC 2010–31017, Calgary, Canada. Doi: https://doi.org/10.1115/IPC2010-31017

International Energy Agency Technology roadmap: high-efficiency. Low-Emissions Coal-Fired Power Generation, Paris, France (2012).

Iredi S, Merkle D (2001) Middendorf M.Bi-criterion optimization with multi colony ant algorithms. In: Zitzler E, et al. editors. Proceedings of the Evolutionary Multi-Criterion Optimization, First International Conference (EMO'01) Vol. 1993 of LNCS. Berlin, Germany: Springer-Verlag: 359–72.

Kashani A, Hesam A, Molaei R (2014) Techno-Economical and Environmental Optimization of Natural Gas Network Operation. Chem Eng Res Des. https://doi.org/10.1016/j.cherd.2014.02.006

Maniezzo V, Colorni A, Dorigo M (1994) The ant system applied to the quadratic assignment problem, Technical Report IRIDIA/94-28. Universit'e Libre de Bruxelles, and Belgium, IRIDIA

Menon ES (2005) Gas pipeline hydraulics. CRC Press, Taylor & Francis Group, Boca Raton, Florida

Mikolajková M, Haikarainen C, Saxén H, Pettersson F (2017) Optimization of a natural gas distribution network with potential future extensions. Energy. https://doi.org/10.1016/j.energy.2016.11.090

Mohring J, Hoffmann J, Hoffmann T, Zemitis A, Basso G, Lagoni P (2004) Automated model reduction of complex gas pipeline network. In Proceedings of the 36th Annual Meeting of Pipeline Simulation Interest Group, California: Palm Springs

Molaei R, Ebrahimi M, Sadeghian S, Fahimnia B (2007) Genetic algorithm optimization of fuel consumption in compressor stations. 3rd WSEAS International Conference on Applied and Theoretical Mechanics, Spain

Montoya SJ, Jovel WA, Hernandez JA, Gonzalez C (2000) Genetic algorithms applied to the optimum design of gas transmission network. SPE International Petroleum Conference and Exhibition, Mexico

OECD (2012) Environmental outlook to 2050: the consequences of inaction. OECD Publishing: Paris 2012

Osiadacz A, Chaczykowski M (2001) Comparison of isothermal and non-isothermal pipeline gas flow models. Chem Eng J 81(1–3):41–51

Osiadacz AJ, Isoli N (2020) Multi-objective optimization of gas pipeline networks. Energies 13(19):5141

Osiadacz AJ (1994) Dynamic optimization of high-pressure gas networks using hierarchical systems theory. 26th annual meeting of Pipeline Simulation Interest Group, Sandiego, CA

Pambour KA, Bolado-Lavin R, Dijkema GPJ (2016) An integrated transient model for simulating the operation of natural gas transport systems. J Nat Gas Sci Eng. https://doi.org/10.1016/j.jngse.2015.11.036

Qin AK, Huang VL, Suganthan PN (2009) Differential evolution algorithm with strategy adaptation for global numerical optimization. IEEE Trans. Evol. Comput. 13, 398e417

Ríos-Mercado RZ, Borraz-Sánchez C (2015) Optimization problems in natural gas transportation systems: a state-of-the-art review. Appl Energy 147:536–555

Schlueter M (2012) Nonlinear mixed integer-based optimization technique for space application, Ph.D. Thesis. University of Birmingham

Smith J, Van Ness H (1998) Introduction to chemical engineering thermodynamics, 4th edn. McGraw-Hill Book Company, Singapore

Socha K, Blum C (2006) Ant colony optimization. In: Alba E, Mart'I R (eds) Metaheuristic procedures for training neural networks, computer science interfaces series. Springer-Verlag, Berlin, Germany, pp 153–180

Stutzle T, Hoos HH (2000) MAX-MIN ant system. Future Generation Comput Syst 16(8):889–914

Tabkhi F, Azzaro-Pantel C, Pibouleau L, Domenech S (2008) A mathematical framework for modeling and evaluating natural gas pipeline networks under hydrogen injection. Int J Hydrog Energy 33:5859–6400

Tabkhi F (2007) Optimization of gas transmission networks. Ph.D. Thesis, France

Thakur AK, Arya AK, Sharma P (2020) The science of alternating current-induced corrosion: a review of literature on pipeline corrosion-induced due to high-voltage alternating current transmission pipelines. Corros Rev 38(6):463–472

Thakur AK, Arya AK, Sharma P (2021) Analysis of cathodically protected steel pipeline corrosion under the influence of alternating current. Materials Today: Proceedings

Üster H, Dilaveroğlu Ş (2014) Optimization for design and operation of natural gas transmission networks. Appl Energy 133:56–69

Wong PJ, Larson RE (1968) " Optimization of Natural- Gas Pipeline System via Dynamic Programming," IEEE Transactions on Automatic Control, Vol 13, No.5, pp.475–481

Wright S, Somani M, Ditzel, C (1988) Compressor station optimization, PSIG, Paper 9805

Wu S, Rios- Mercado RZ, Boyd EA, Scott LR (2000) Model relaxations for the fuel cost minimization of steady-state gas pipeline networks. Math Comput Modell 31(2):197–220

Xia X, Gui L, He G, Wei B, Zhang Y, Yu F, Wu H, Zhan ZH (2020) An expanded particle swarm optimization based on multi-exemplar and forgetting ability. Inf Sci 508:105–120

Yang X, Li H, Wallin F, Zhixin Yu, Wang Z (2017) Impacts of emission reduction and external cost on natural gas distribution. Appl Energy 207:553–561

Zheng, Qipeng P, Steffen R, Niko AI, Panos MP (2010) "Optimization Models in The Natural Gas Industry." In *Handbook of Power Systems I*, Doi: https://doi.org/10.1007/978-3-642-02493-1_6